Available online at www.sciencedirect.com
SCIENCE DIRECT
ELSEVIER
Icarus 177 (2005) 447–460
ICARUS
www.elsevier.com/locate/icarus

# Convective–conductive transitions and sensitivity of a convecting ice shell to perturbations in heat flux and tidal-heating rate: Implications for Europa

Giuseppe Mitri [a,b,*], Adam P. Showman [a]

[a] *Department of Planetary Sciences, Lunar and Planetary Laboratory, University of Arizona, Tucson, AZ, USA*
[b] *International Research School of Planetary Sciences, University G. d'Annunzio, Pescara, Italy*

Received 17 July 2004; revised 29 January 2005

Available online 26 May 2005

**Abstract**

We investigate the response of conductive and convective ice shells on Europa to variations of heat flux and interior tidal-heating rate. We present numerical simulations of convection in Europa's ice shell with Newtonian, temperature-dependent viscosity and tidal heating. Modest variations in the heat flux supplied to the base of a convective ice shell, $\Delta F$, can cause large variations of the ice-shell thickness $\Delta\delta$. In contrast, for a conductive ice shell, large $\Delta F$ involves relatively small $\Delta\delta$. We demonstrate that, for a fluid with temperature-dependent viscosity, the heat flux undergoes a finite-amplitude jump at the critical Rayleigh number $Ra_{cr}$. This jump implies that, for a range of heat fluxes relevant to Europa, two equilibrium states—corresponding to a thin, conductive shell and a thick, convective shell—exist for a given heat flux. We show that, as a result, modest variations in heat flux near the critical Rayleigh number can force the ice shell to switch between the thin, conductive and thick, convective configurations over a $\sim 10^7$-year interval, with thickness changes of up to ~10–30 km. Depending on the orbital and thermal history, such switches might occur repeatedly. However, existing evolution models based on parameterized-convection schemes have to date not allowed these transitions to occur. Rapid thickening of the ice shell would cause radial expansion of Europa, which could produce extensional tectonic features such as fractures or bands. Furthermore, based on interpretations for how features such as chaos and ridges are formed, several authors have suggested that Europa's ice shell has recently undergone changes in thickness. Our model provides a mechanism for such changes to occur.


*Keywords:* Europa; Geophysics; Ices; Interiors; Satellites of Jupiter; Thermal convection; Thermal histories

## 1. Introduction

We investigate the response of a conductive and convective ice shell to changes of heat production in the silicate mantle and in the ice shell of Jupiter's satellite Europa. Estimates of Europa's ice-shell thickness range from ~3 to 50 km (Turtle and Ivanov, 2002; Schenk, 2002; Hussmann et al., 2002; Tobie et al., 2003; Williams and Greeley, 1998; Greenberg et al., 1998, 1999). This uncertainty in thickness translates directly into an uncertainty in the heat-transfer mechanism: if the shell is thick, the rigid surface could be underlain by a layer of convecting water ice (Cassen et al., 1979; McKinnon, 1999; Pappalardo et al., 1998; Showman and Han, 2004; Tobie et al., 2003), whereas a thin shell would instead transport the heat by conduction (Greenberg et al., 1998, 1999). Interestingly, most estimates of the shell thickness (10–40 km) imply that the ice-shell Rayleigh number is near the critical Rayleigh number, which is $\sim 10^6$ for realistic temperature-dependent viscosities (e.g., McKinnon, 1999).

The implications of surface landforms for the configuration of the ice shell remain controversial (Pappalardo et

* Corresponding author.
*E-mail addresses:* mitri@lpl.arizona.edu (G. Mitri), showman@lpl.arizona.edu (A.P. Showman).

0019-1035/$ – see front matter 
doi:10.1016/j.icarus.2005.03.019

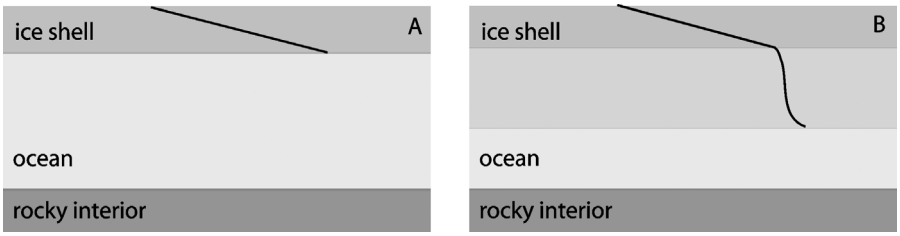


Fig. 1. Structures and temperature profiles for two possible configurations of the ice shell of Europa. The heat generated in the interior of the planet might be shed by simple conduction through a relatively thin ice shell directly overlying a subsurface ocean (A), or transported equally well through a much thicker ice shell containing of an actively convecting layer (B). Because of the large viscosity near the surface, the ice shell in B develops a stagnant lid at the surface; the convective motions are confined to a sublayer of the ice shell. The states (A) and (B) could have very similar heat fluxes.

al., 1999). Numerous small (3–30-km diameter) pits, uplifts, and disrupted spots, as well as larger chaos terrains such as Conamara Chaos and the Mitten, have been attributed to convection in an ice shell at least 10-km thick (Pappalardo et al., 1998; Head and Pappalardo, 1999; Collins et al., 1999, 2000; Figueredo et al., 2002). But other authors have suggested that chaos results instead from melt-through of a thin ice shell (Williams and Greeley, 1998; Greenberg et al., 1999, 2003; O'Brien et al., 2002; Melosh et al., 2004). Similarly, some formation mechanisms for ridges require a thin-ice shell (Greenberg et al., 1998), while other ridge-formation mechanisms allow a thicker shell (Melosh and Turtle, 2004; Nimmo and Gaidos, 2002). Figueredo and Greeley (2004), Prockter et al. (1999), Pappalardo et al. (1999), and others have shown that tectonic resurfacing (i.e., ridge building) decreased rapidly after ridged-plains formation and that chaos formation has increased with time. These authors suggest that the transition from tectonic- to chaos resurfacing resulted from the gradual thickening of the ice shell. On the other hand, Greenberg et al. (1999, 2000, 2003) suggests a different scenario where the chaos and tectonic terrains form concurrently and continually resurface Europa.

Fig. 1 shows the schematic structures and temperature profiles for the two plausible configurations of the ice shell (conductive and convective). Both structures have a steep temperature gradient within the top layer and lose heat conductively through this layer. Within the conductive regime, heat flux follows a rough inverse proportionality to layer thickness, so thicker layers transport smaller heat fluxes. In layers thicker than a critical value, $\delta_{\rm crit}$, the Rayleigh number exceeds the critical Rayleigh number, and convection begins. The assumption is often made that the heat flux near this transition is a continuous function of the layer thickness. In this case, the heat flux of the conductive solution (A) would exceed that of the convective solution (B). However, laboratory experiments in a fluid with temperature-dependent viscosity indicate that, at the critical Rayleigh number, the convection jumps directly to a finite-amplitude regime (Stengel et al., 1982), implying that the heat flux for a convective layer infinitesimally thicker than $\delta_{\rm crit}$ *exceeds* that for a conductive layer infinitesimally thinner than $\delta_{\rm crit}$. This implies that the heat flux for a convective layer infinitesimally thicker than $\delta_{\rm crit}$ will be *equal* to the heat flux for a conductive state that is substantially thinner than $\delta_{\rm crit}$. Therefore, for a range of conditions near the critical Rayleigh number, two solutions—one a thin, conductive shell and the other a thick, convective shell—exist for a given basal heat flux. The existence of two solutions for a given heat flux raises an obvious question: What determines which of the two states Europa occupies? And can Europa switch between these states? Furthermore, in the convective regime, how sensitive is the ice-shell thickness to perturbations in the basal heat flux and internal tidal-heating rate? Answers to these questions have important implications for the time history of Europa's ice-shell thickness, and hence for Europa's surface geology.

These questions become even more relevant considering that Europa's heat-production rate may vary in time. Io's measured heat flux exceeds that possible in steady state, which may result from $\sim 10^8$ year oscillations in Io's eccentricity and tidal-heating rate caused by coupled orbital-geophysical feedbacks (Greenberg, 1982; Ojakangas and Stevenson, 1986). Similar feedbacks may be relevant for Ganymede (Showman et al., 1997) and Europa (Hussmann and Spohn, 2004). (In any case, oscillations of Io's eccentricity would cause oscillations in Europa's eccentricity and tidal-heating rate even in the absence of any feedbacks in Europa.) The observational suggestion that Europa's geology has shifted from ridge to chaos formation over the past 50 Myr (Pappalardo et al., 1999; Prockter et al., 1999; Greeley et al., 2000; Kadel et al., 2000; Figueredo and Greeley, 2004) supports the idea that variations in Europa's internal heating rate and ice-shell thickness have occurred over time.

Here we present two-dimensional numerical simulations of convection in Europa's ice shell, including tidal heating, to investigate the sensitivity of the ice-shell thickness to perturbations in basal heat flux and interior tidal-heating rate. Our simulations confirm Stengel et al.'s (1982) result that the heat flux undergoes a finite-amplitude jump at the critical Rayleigh number; furthermore, this occurs at heat fluxes relevant to Europa ($\sim$0.02–0.06 $\mathrm{W\,m^{-2}}$ depending on the viscosity and tidal-heating rate). We determine the amplitude of the heat-flux jump and discuss the consequences for the thermal evolution of the ice shell. We show that, if the system is near the critical Rayleigh number, small changes in the heat flux can force the system to switch from conductive to convective configurations with large variations in

thickness of the ice shell. The consequent volume changes of Europa can generate surface stresses up to ∼100 bar, potentially causing formation of fractures, bands, or other structures. The direct jump to *finite-amplitude* convection also increases the likelihood that convection can disrupt the surface even when the Rayleigh number is barely supercritical, which may help to allow the production of chaos, pits, and uplifts soon after initiation of convection in a gradually thickening ice shell (as has been suggested by several authors). The models presented here may also have applicability for the thermal evolution of Ganymede, Callisto, Titan, and the small icy moons of Saturn and Uranus.

## 2. Model

We consider a model of an ice shell overlying a global ocean. The Boussinesq fluid equations are solved with the ConMan finite-element code (King et al., 1990). The code solves the dimensionless equations of momentum, continuity and energy, respectively given by (e.g., Schubert et al., 2001)

$$\frac{\partial \sigma_{ij}}{\partial x_j} + Ra\vartheta k_i = 0, \tag{1}$$

$$\frac{\partial u_i}{\partial x_i} = 0, \tag{2}$$

$$\frac{\partial \vartheta}{\partial t} + u_i \frac{\partial \vartheta}{\partial x_i} = \frac{\partial^2 \vartheta}{\partial x_i^2} + Q, \tag{3}$$

where $\sigma_{ij}$ is the dimensionless stress tensor, $u_i$ is the dimensionless velocity, $\vartheta$ is dimensionless temperature, $k_i$ is the vertical unit vector, $t$ is dimensionless time, $x_i$ and $x_j$ are the dimensionless spatial coordinates, and $i$ and $j$ are the coordinate indices. $Q$ is the dimensionless volumetric heating rate. The nondimensionalization is performed using length, speed, and time scales of $\delta$, $\kappa/\delta$, and $\delta^2/\kappa$, respectively, where $\delta$ is the ice-shell thickness, and $\kappa$ is the thermal diffusivity.

The stresses in dimensional form are given by

$$\sigma_{ij} = -p\delta_{ij} + \eta\left(\frac{\partial u_i}{\partial x_j} + \frac{\partial u_j}{\partial x_i}\right), \tag{4}$$

where $p$ is the pressure, $\delta_{ij}$ is the Kronecker delta, and $\eta$ is the temperature-dependent viscosity. The Rayleigh number $Ra$ is given by

$$Ra = \frac{\alpha_{\rm ice}\rho g \Delta T \delta^3}{\kappa \eta_0}, \tag{5}$$

where $g$ is gravitational acceleration (1.32 m s$^{-2}$), $\alpha_{\rm ice}$ is the coefficient of thermal expansion ($1.6 \times 10^{-4}$ K$^{-1}$), $\kappa$ is the thermal diffusivity of the water ice ($1.0 \times 10^{-6}$ m$^2$ s$^{-1}$), $\rho$ is the density of the water ice (917 kg m$^{-3}$), $\Delta T$ is the temperature difference between the bottom and the top surfaces, and $\eta_0$ is the viscosity of the water ice at the melting point ($10^{13}$–$10^{15}$ Pa s). The physical parameters used in the model are summarized in Table 1.

Table 1
Physical parameters

| | | |
|---|---|---|
| Thermal expansivity of ice | $\alpha_{\rm ice}$ | $1.6 \times 10^{-4}$ K$^{-1}$ |
| Gravitational acceleration | $g$ | 1.32 m s$^{-2}$ |
| Thermal diffusivity of ice | $\kappa$ | $1.3 \times 10^{-6}$ m$^2$ s$^{-1}$ |
| Thermal conductivity of ice | $k$ | 2.3 W m$^{-1}$ K$^{-1}$ |
| Ice density | $\rho$ | 917 kg m$^{-3}$ |
| Surface temperature | $T_{\rm s}$ | 95 K |
| Melting temperature of ice | $T_{\rm m}$ | 270 K |
| Ice viscosity at $T_{\rm m}$ | $\eta_0$ | $10^{13}$–$10^{15}$ Pa s |
| Europa radius | $R$ | 1569 km |
| Orbital frequency | $\omega$ | $2 \times 10^{-5}$ s$^{-1}$ |
| Rigidity of ice | $\mu$ | 3–4 $\times 10^9$ Pa |

The surface temperature is held at $T_{\rm s} = 95$ K and the bottom temperature of the ice shell is fixed at the melting temperature of fresh water, $T_{\rm m} = 270$ K. The numerical simulations are performed in a Cartesian domain, which is a good approximation for Europa's ice shell because its thickness is much less than the radius of the satellite. Most simulations used a resolution of 190 × 48 finite elements, but the resolution was increased to 190 × 100 elements for the high Rayleigh number cases. This improved resolution is needed to resolve the fine-scale convective structure, and obtain proper estimates of the heat flux, for the high-Rayleigh-number cases. The highest-Rayleigh-number cases ($Ra = 10^9$) were rerun at 200 × 200 to verify numerical convergence of the heat fluxes. The velocity boundary conditions are periodic on the sides and free-slip rigid walls on the top and the bottom of the domain. The domain has a width:height ratio of 4:1, which is large enough to minimize the influence of the domain on the convective structure. Selected cases were also rerun at a width:height ratio of 6:1 to verify that (consistent with the findings of Solomatov and Moresi, 2000) the domain has minimal influence on the results. The simulations are initialized using a conductive temperature profile containing a sinusoidal thermal perturbation with an amplitude of 0.175 K.

Goldsby and Kohlstedt (2001) proposed a composite constitutive equation to account for the combined strain rate $\dot{\varepsilon}$ of several deformation mechanisms as follows:

$$\dot{\varepsilon} = \dot{\varepsilon}_{\rm diff} + \left(\frac{1}{\dot{\varepsilon}_{\rm basal}} + \frac{1}{\dot{\varepsilon}_{\rm gbs}}\right)^{-1} + \dot{\varepsilon}_{\rm disl}, \tag{6}$$

where $\dot{\varepsilon}_{\rm diff}$, $\dot{\varepsilon}_{\rm basal}$, $\dot{\varepsilon}_{\rm gbs}$, $\dot{\varepsilon}_{\rm disl}$ are strain rate of diffusional flow, basal slip, grain boundary sliding, and dislocation creep, respectively. The strain rate for a single mechanism $\dot{\varepsilon}_j$ can be described by

$$\dot{\varepsilon}_j = A\frac{\sigma^n}{d^p}\exp\left(-\frac{Q^*}{\mathcal{R}T}\right), \tag{7}$$

where $d$ is the grain size, $\sigma$ is the shear stress, $A$, $n$, and $p$ are constants, $Q^*$ is the activation energy, $\mathcal{R}$ is the gas constant, and $T$ is temperature (Goldsby and Kohlstedt, 2001). The flow law parameters are in Table 2. The diffusion creep

Table 2
Flow law parameters (Goldsby and Kohlstedt, 2001)

| Creep regime | $A$ | $n$ | $Q^*$ (kJ mol$^{-1}$) | $p$ |
|---|---|---|---|---|
| Dislocation creep ($T < 258$ K) | $4.0 \times 10^5$ MPa$^{-4.0}$ s$^{-1}$ | 4.0 | 60 | 0 |
| Dislocation creep ($T > 258$ K) | $6.0 \times 10^{28}$ MPa$^{-4.0}$ s$^{-1}$ | 4.0 | 180 | 0 |
| GBS ($T < 255$ K) | $3.9 \times 10^{-3}$ MPa$^{-1.8}$ m$^{1.4}$ s$^{-1}$ | 1.8 | 49 | 1.4 |
| GBS ($T > 255$ K) | $3.0 \times 10^{26}$ MPa$^{-1.8}$ m$^{1.4}$ s$^{-1}$ | 1.8 | 192 | 1.4 |
| Basal slip | $5.5 \times 10^7$ MPa$^{-1.8}$ s$^{-1}$ | 2.4 | 60 | 0 |

rate is calculated using the equation (Goldsby and Kohlstedt, 2001)

$$\dot{\varepsilon} = \frac{42\sigma V_\mathrm{m}}{\mathcal{R}Td^2}\left(D_\mathrm{v} + \frac{\pi\delta_\mathrm{g}}{d}D_\mathrm{b}\right), \tag{8}$$

where $V_\mathrm{m}$ is the molar volume ($1.97 \times 10^{-5}$ m$^3$), $\delta_\mathrm{g}$ is the grain boundary width ($9.04 \times 10^{-10}$ m), and $D_\mathrm{v}$ and $D_\mathrm{b}$ are volume and grain boundary diffusion coefficients, respectively, each of the form $D_i = D_{0,i}\exp(\frac{Q^*}{\mathcal{R}T})$. Goldsby and Kohlstedt (2001) assumed that $Q^* = 49$ kJ mol$^{-1}$ and the preexponent term for grain boundary diffusion is equivalent to that for volume diffusion ($9.10 \times 10^{-4}$ m$^2$ s$^{-1}$). The predominant creep mechanisms under conditions relevant to a convecting ice shell are superplastic deformation with grain boundary sliding (GBS) in combination with diffusion motion (Table 3) (McKinnon, 1999; Goldsby and Kohlstedt, 2001; Durham et al., 1997). McKinnon (1998, 1999) argued that the thermal-buoyancy stress is $\sim 0.1\rho g\alpha\Delta T_\mathrm{plume}\delta$, where $\Delta T_\mathrm{plume} \sim 5$ K is the temperature difference between warm and cold plumes. For Europa, this scaling implies convective stresses of $\sim 10^{-2}$–$10^{-3}$ MPa, whereas the expected tidal stress ~0.01–0.1 MPa, depending on the ice-shell temperature. McKinnon (1999) suggested that if $\sigma_\mathrm{conv} \ll \sigma_\mathrm{tid}$, the tidal stresses act to linearize the viscosity, eliminating the dependence of viscosity on the convective stress even for non-Newtonian creep mechanisms. Nevertheless, the stresses are uncertain and it is possible that convective and tidal stresses are comparable. Even in this case, however, the fact that GBS is only mildly non-Newtonian implies that the viscosity varies by only a factor of ~2–5 with plausible variations in stress, which is much smaller than the orders-of-magnitude viscosity variations associated with changes in temperature (e.g., Showman and Han, 2004). Consequently, here we assume that the viscosity is Newtonian, and we defer exploration of non-Newtonian rheologies to future work. The Newtonian temperature dependent viscosity of the water ice is given by

$$\eta = \eta_0 \exp\left[A^*\left(\frac{T_\mathrm{m}}{T} - 1\right)\right]. \tag{9}$$

We use a value of the constant $A^* = 7.5$, which yields a viscosity contrast $\Delta\eta$, defined as the ratio between the maximum and the minimum viscosities in the simulation, of $\Delta\eta = 10^6$. This value is chosen to maintain the convection in the stagnant-lid regime (e.g., Solomatov and Moresi, 2000) while ensuring that the viscosity contrast across each finite element is less than a factor of ~2, as necessary to maintain numerical accuracy (Moresi et al., 1996). Although the actual viscosity contrast far exceeds $10^6$, we expect that our simulations preserve the essential aspects of the convective behavior. Larger values of $A^*$ would lead to larger values of the critical Rayleigh number, which would increase the minimum ice-shell thickness for convection to initiate. The *qualitative* existence of a heat-flux jump at the critical Rayleigh number should not be affected, however (in fact, we expect that our simulations at artificially small $\Delta\eta$ *underestimate* the amplitude of the heat-flux jump at the critical Rayleigh number).

For this preliminary study, we ignore the pressure-dependence of the melting temperature, which is approximately valid for ice shells thinner than 50 km, relevant to Europa. Pressure-dependence of the melting temperature is more likely to play a role for satellites with thicker ice shells such as Ganymede, Callisto, or Titan. The possible presence of salts and ammonia in the ocean may reduce the melting temperature of the ice by up to a few K for plausible compositions (e.g., Kargel, 1991); however, in this model we neglect this effect and maintain the basal temperature at 270 K.

The thermal conductivity of ice depends on the temperature, but ConMan assumes constant conductivity. The convecting sublayer remains nearly isothermal, and most of the temperature variation occurs within the stagnant lid. We therefore expect that constant-conductivity simulations provide reasonably accurate solutions throughout the convection region; the primary effect of variable conductivity

Table 3
Strain rates of diffusion flow, basal slip, grain boundary sliding, dislocation creep, and the total strain rate using the composite constitutive equation for different grain size of the water ice in the tidal stress range ($10^4$–$10^5$ Pa). The creep mechanism that likely contributes most to the strain rate on Europa conditions of the ice shell is the superplastic flow regime with grain boundary sliding (GBS) deformation process in combination with diffusion motion

| Grain size | 0.001 m | 0.001 m | 0.00001 m | 0.00001 m |
|---|---|---|---|---|
| Stress | $10^4$ Pa | $10^5$ Pa | $10^4$ Pa | $10^5$ Pa |
| Dislocation creep | $1.1 \times 10^{-15}$ | $1.1 \times 10^{-11}$ | $1.1 \times 10^{-15}$ | $1.1 \times 10^{-11}$ |
| GBS | $8.5 \times 10^{-13}$ | $5.4 \times 10^{-11}$ | $5.4 \times 10^{-10}$ | $3.4 \times 10^{-8}$ |
| Basal slip | $2.4 \times 10^{-10}$ | $6.1 \times 10^{-8}$ | $2.4 \times 10^{-10}$ | $6.6 \times 10^{-8}$ |
| Diffusion | $1.3 \times 10^{-12}$ | $1.3 \times 10^{-11}$ | $1.3 \times 10^{-8}$ | $1.3 \times 10^{-7}$ |
| Total | $2.1 \times 10^{-12}$ | $7.8 \times 10^{-11}$ | $1.3 \times 10^{-8}$ | $1.5 \times 10^{-7}$ |

would be to alter the thickness of the stagnant lid by ∼50% for a given heat flux (see Tobie et al., 2003 for discussion).

We include temperature-dependent internal tidal heating in the numerical model. We use the volumetric dissipation rate for an incompressible Maxwell body, which can be written

$$q = \frac{\varepsilon_0^2 \omega^2 \eta}{[1 + \frac{\omega^2 \eta^2}{\mu^2}]}, \tag{10}$$

where $\omega = 2 \times 10^{-5}$ s$^{-1}$ is the europan orbital frequency, $\mu = 3 \times 10^9$ Pa is the rigidity of the water ice, and $\varepsilon_0$ is the maximum magnitude of tidal-flexing strain of the ice shell during Europa's orbit around Jupiter. The temperature dependence of $q$ is determined by the temperature dependence of the ice viscosity given by Eq. (9). A simple estimate of $\varepsilon_0$ is given by the ratio $\xi/R$ between the amplitude of the vertical surface deformation $\xi$ during a tidal cycle (20–30 m) (Ross and Schubert, 1987; Moore and Schubert, 2000) and the radius of Europa ($R = 1569$ km). The tidal flexing amplitude $\varepsilon_0$ ranges from $1 \times 10^{-5}$ to $2 \times 10^{-5}$ (Showman and Han, 2004).

At high Rayleigh numbers, the heat flux through the top and bottom boundaries fluctuates in time and space (e.g., Tobie et al., 2003). For our analysis, we calculated the local heat flux from the thermal gradient at the boundary and spatially and temporally averaged this heat flux to obtain the mean heat flux. The heat-flux calculations were performed after the flows reached a statistical equilibrium (after the initial start-up transient was finished). The temporal averaging was performed using 10–15 output frames over ∼1–5 × 10$^5$, ∼5 × 10$^5$–1 × 10$^6$, and ∼2–8 × 10$^6$ year-periods for $\eta_0 = 10^{13}$, $10^{14}$, and $10^{15}$ Pa s, respectively. These averaging times are all longer than the convective overturn times of ∼10$^4$–10$^5$ years for $\eta_0 = 10^{13}$–$10^{15}$ Pa s.

The ConMan code assumes that the ice-layer thickness $\delta$ is constant throughout each simulation, so there is no direct way to account for ice-shell thickness fluctuations in response to thermal perturbations. Therefore, we cannot explicitly simulate a convective-conductive switch—with the associated ice-shell thickness changes—within any given ConMan simulation. However, we can perform constant-thickness simulations to determine the equilibrium heat flux for a given shell thickness and tidal-flexing amplitude; we then use these results to *infer* how the thickness will change if the basal heat flux or tidal-flexing amplitude change. This approach is valid as long as the perturbations in heat flux or tidal-flexing amplitude occur on timescales long compared to the convective timescale $\tau_{\rm conv}$, which is $10^4$–$10^5$ years for viscosities of $10^{13}$–$10^{15}$ Pa s. Even near the critical Rayleigh number, where the equilibration times are longer because of the smaller role of advection relative to conduction, the heat fluxes in our simulations equilibrate within ∼2 × 10$^6$–3 × 10$^7$ years for melting-point viscosities of $10^{13}$–$10^{15}$ Pa s. In contrast, the expected changes in shell thickness associated with coupled orbital–geophysical feedbacks are ∼10$^7$–10$^8$ years (e.g., Ojakangas and Stevenson, 1986; Showman et al., 1997; Hussmann and Spohn, 2004). Therefore, the constant-thickness simulations provide an approximately correct description of the convection, at least for $\eta_0 \leqslant 10^{14}$ Pa s.

## 3. Results and discussion

### 3.1. Basic morphology of the convection

In agreement with earlier investigations (McKinnon, 1999; Wang and Stevenson, 2000; Sotin et al., 2002; Barr and Pappalardo, 2003; Showman and Han, 2004; Tobie et al., 2003), our results demonstrate that convection can occur under conditions relevant to Europa (Figs. 2 and 3). For an ice shell without internal heating, convection can occur in ice shells thicker than 10 and 21 km for melting-temperature viscosities of $10^{13}$ and $10^{14}$ Pa s, respectively. In a tidally heated ice shell with tidal-flexing amplitude $\varepsilon_0 \sim 1$–$2 \times 10^{-5}$, convection can occur in layers thicker than 9 and 19 km for melting-temperature viscosities of $10^{13}$ and $10^{14}$ Pa s, respectively. The critical Rayleigh number $Ra_{\rm cr}$ depends on tidal-heating rate, and is smaller when

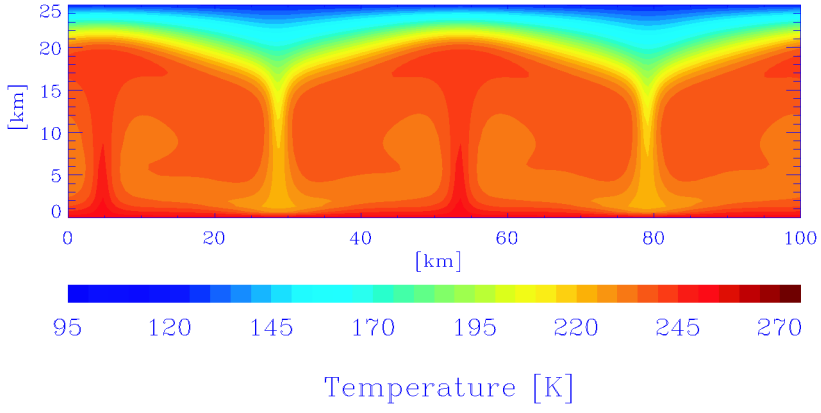


Fig. 2. Temperature field of a numerical simulation without internal heating in the ice shell. The domain is 25 km thick and 100 km wide. The melting point viscosity is $10^{13}$ Pa s and the basal Rayleigh number is $5.2 \times 10^7$. The time of this frame is $1.2 \times 10^7$ yr.

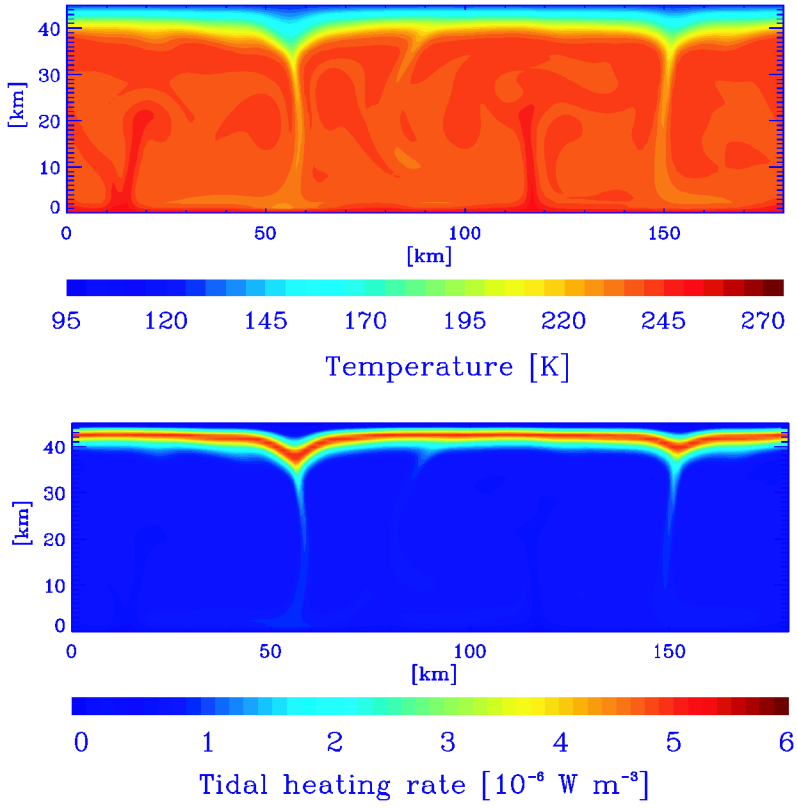


Fig. 3. Temperature field of a numerical simulation with internal heating in the ice shell. The domain is 45 km thick and 180 km wide. The melting point viscosity is $10^{13}$ Pa s and the basal Rayleigh number is $5.6 \times 10^8$. The tidal flexing amplitude of the ice shell is $\varepsilon_0 = 1.5 \times 10^{-5}$. The time of this frame is $1.2 \times 10^7$ yr.

the tidal heating is larger. As expected, the temperature-dependence of the viscosity leads to formation of a 4–8-km thick stagnant lid at the surface; in contrast, the boundary layer at the bottom of the system is only 1–2-km thick and actively participates in the convection (Solomatov, 1995; Moresi and Solomatov, 1995; McKinnon, 1999; Deschamps and Sotin, 2001; Solomatov and Moresi, 2000; Showman and Han, 2004; Tobie et al., 2003). For $Ra <$ 1–5 $\times$ $10^7$, depending on the tidal-heating rate, the convection is steady-state, with periodic, regularly spaced upwellings and downwellings (Fig. 2). For Rayleigh numbers greater than this value, the convection is time dependent and lacks the regular symmetry of the steady-state regime (Fig. 3). The bottom panel of Fig. 3 illustrates that the tidal-heating rate depends on temperature. For $\eta_0 = 10^{13}$ Pa s, the magnitude of tidal heating is greatest along the base of the stagnant lid and within cold descending plumes (Fig. 3b); in contrast, for $\eta_0 = 10^{14}$ Pa s the greatest heating occurs at the bottom of the ice shell and in hot ascending plumes (e.g., Wang and Stevenson, 2000; Sotin et al., 2002).

### 3.2. Nusselt number–Rayleigh number relationship

The Nusselt number, defined as

$$Nu = \frac{F\delta}{k\Delta T}, \tag{11}$$

where $F$ is the heat flux, provides a measure of how vigorously the convection transports heat. Analytical investigations of internally or basally heated fluids suggest a relationship between the Nusselt number Nu and the Rayleigh number $Ra_i$, evaluated using a characteristic viscosity in the interior of the convective sublayer, given by (Morris and Canright, 1984; Fowler, 1985)

$$Nu = \alpha {Ra_i}^{\beta} \theta^{\gamma}, \tag{12}$$

where $\theta \equiv -\partial \ln \eta / \partial T$ characterizes the temperature-dependence of the viscosity. The coefficients $\alpha$, $\beta$, and $\gamma$ are dimensionless constants that depend on the boundary conditions of the convective system (Turcotte and Oxburgh, 1967; Roberts, 1979; Howard, 1964; Somerscales and Gazda, 1968; Dropkin and Somerscales, 1965; Goldstein et al., 1990). For the steady-state convection regime at low Rayleigh number, Dumoulin et al. (1999) suggest parameter values of $\alpha = 1.99$, $\beta = 1/5$, and $\gamma = -1$, and for the time-dependent regime at high Rayleigh number $\alpha = 0.52$, $\beta = 1/3$, and $\gamma = -4/3$. Between the stationary and the time-dependent regimes, there is a time-dependent transitional regime that has parameters $\alpha$, $\beta$, and $\gamma$ equal to the values for the stationary regime. These values are generally consistent with values suggested by Moresi and Solomatov (1995), Davaille and Jaupart (1993), and others; see Solomatov and Moresi (2000) for a summary.

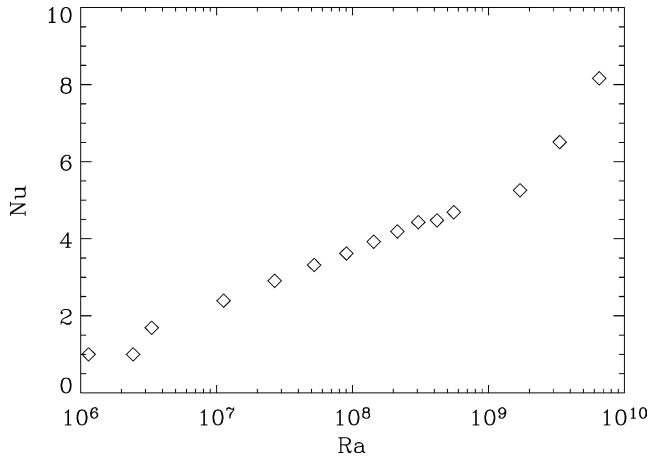


Fig. 4. Relation between the basal Rayleigh number Ra and the Nusselt number Nu for an ice shell without internal heating. The figure shows a finite amplitude jump of Nusselt number at the critical Rayleigh number ($3 \times 10^6$). The relationship between Ra and Nu has two different trends for low and high Ra.

Fig. 4 shows the Nu–Ra relationship obtained from a broad range of our simulations. The figure illustrates that at $Ra \sim 10^9$, a break in the slope occurs; the power-law exponent $\beta$ is about 1/3 for $Ra > 10^9$ and 1/5 for $3 \times 10^6 < Ra < 10^9$. These results broadly agree with the theories summarized above. The $\beta \approx 1/5$ regime encompasses both steady-state convection at low $Ra$ ($<$1–5 $\times$ $10^7$) as well as time-dependent convection at higher $Ra$ ($>5 \times 10^7$); in other words, the transition between steady-state and time-dependent convection occurs at lower Rayleigh number than the transition between the $\beta \approx 1/5$ and $\beta \approx 1/3$ regimes. Interestingly, the transition between the $\beta \approx 1/5$ and 1/3 regimes occurs at $Nu \sim 5$, which agrees with the results of Dumoulin et al. (1999). However, we expect that the value of $Ra$ at this transition depends on the viscosity contrast; greater viscosity contrasts imply a lower value of $Ra$ at the $\beta \approx 1/5$–1/3 transition (Dumoulin et al., 1999). At Rayleigh numbers less than the critical Rayleigh number of $\sim 3 \times 10^6$, the shell loses heat purely by conduction, corresponding to $Nu = 1$.

In the $\beta \approx 1/3$ regime, the heat flux is essentially independent of ice-shell thickness, which implies that the ice-shell thickness is extremely sensitive to perturbations in the basal-heat flux. In this regime, infinitesimal decreases in the heat flux supplied to the base of the shell cause complete refreezing of the shell, whereas infinitesimal increases in the heat flux supplied to the base of the shell cause thinning sufficient to force the shell into the $\beta \approx 1/5$ regime (whereupon the ice-shell thickness is no longer so sensitive to basal-heat flux). Given the observational evidence for an ocean (Kivelson et al., 2000), we therefore infer that the ice shell lies within either the $\beta \approx 1/5$ convective regime or the conductive regime. The extreme thickness variations in the coupled orbital–thermal parameterized-convection simulations of Hussmann and Spohn (2004) probably result from their choice of $\beta = 0.3$. In future studies, it may be preferable to use $\beta = 1/5$, which would probably lead—in the convective regime—to more modest ice-shell thickness variations than found by Hussmann and Spohn (2004). Nevertheless, we will show that substantial thickness variations can still accompany switches between convective and conductive states near the critical Rayleigh number.

Interestingly, we find that immediately above the critical Rayleigh number, Nu increases discontinuously to $\sim$1.7, which implies that the convection jumps directly into a finite-amplitude regime (i.e., the convected flux is 70% of the conducted flux, rather than an infinitesimal fraction as would be predicted by linear theory). This result agrees with laboratory experiments using glycerol conducted by Stengel et al. (1982), who found that the Nusselt number at the critical Rayleigh number ranged from 1.1 to 1.2 for viscosity ratios of 150–3400 (and an extrapolation of his results to viscosity contrasts of $10^6$ suggests $Nu = 1.7 \pm 0.5$ at the critical Rayleigh number, consistent with our results).

We propose the following explanation. At constant viscosity, linear theory predicts broad, domain-filling convection cells, and at weakly supercritical Rayleigh numbers, these cells produce only a minor perturbation to the conductive temperature profile. This behavior implies that a single convection cell, in the linear regime, spans temperatures ranging from that at the bottom to that at the top of the domain (i.e., small-amplitude convection cells are far from isothermal). When the viscosity depends strongly on temperature, however, convection cells cannot a span broad range of temperature, because only the viscosity at the lower boundary is low enough for fluid deformation to occur. This phenomenon initially inhibits convection (leading to higher critical Rayleigh numbers for temperature-dependent-viscosity than for constant-viscosity fluids). For convection to finally begin, the convection cells must immediately jump into an approximately isothermal state with a temperature close to that at the lower boundary. This is a finite-amplitude state, because finite temperature advection must counteract conduction to maintain the isothermal nature of the convection cells. The resulting Nusselt number depends on the thickness of the cells and in turn the viscosity contrast; if the convection cells fill one-third of the domain, the stagnant lid would be two-thirds of the domain thickness and the resulting Nusselt number would be $\sim$1.5. These arguments are broadly consistent with convective scaling theories, which predict finite velocities at the critical Rayleigh number when the viscosity contrast is large (e.g., Solomatov and Moresi, 2000).

### *3.3. Conductive–convective transitions and sensitivity of ice shell to thermal perturbations*

We now describe the dependence of heat flux on shell thickness and discuss the implications for Europa's thermal evolution. Fig. 5 illustrates how the heat flux depends on ice-shell thickness for a sequence of runs with no tidal heating and the parameter values listed in Table 1. Each point rep-

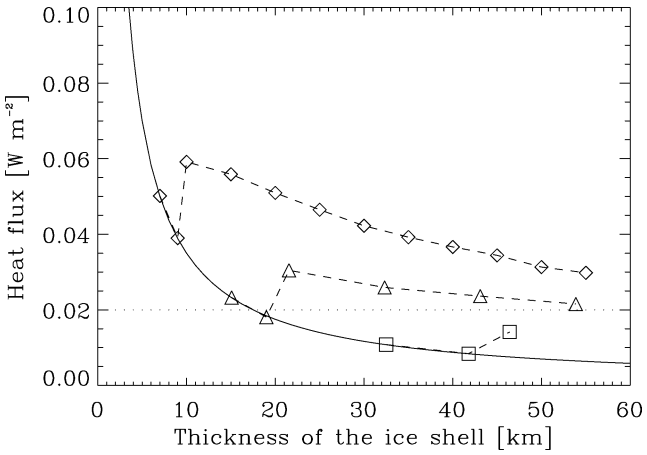


Fig. 5. Relation between the heat flux generated in the silicate mantle and the thickness of the ice shell (in a range 0–60 km) for ice melting-temperature viscosities of $10^{13}$ Pa s (diamonds), $10^{14}$ Pa s (triangles), and $10^{15}$ Pa s (squares). These numerical simulations are without internal heating in the ice shell. The radiogenic heat flux ranges from 0.005–0.020 W m$^{-2}$ (Melosh et al., 2004; Tobie et al., 2003). The maximum radiogenic heat flux is plotted in dashed line.

resents the results of a simulation; diamonds, triangles, and squares correspond to simulations with $\eta_0 = 10^{13}$, $10^{14}$, and $10^{15}$ Pa s, respectively. Because tidal heating was excluded here, the time-averaged fluxes through the top and bottom boundaries are equal. In each case, the plotted flux corresponds to that needed to reach an approximate equilibrium (i.e., statistical steady state) under the constraints of constant ice-shell thickness and bottom-to-top temperature contrast. The solid curve shows the conductive heat flux $F = k\Delta T/\delta$ and the dotted line provides a schematic upper limit to the expected radiogenic heat flux from Europa's interior. (We adopt constant $k$ here for consistency with ConMan, which assumes constant conductivity.) The figure illustrates several important points. First, the thinnest-shell simulations for each value of $\eta_0$ had subcritical Rayleigh numbers and produced conductive solutions; these simulations fall along the solid curve. Simulations that produced convection had total fluxes exceeding the conductive flux; these simulations fall above the solid curve. Second, the heat-flux discontinuity at the critical Rayleigh number is clearly evident; the total flux at Rayleigh numbers just slightly greater than $Ra_{cr}$ is about 1.7 times the corresponding conductive flux. Third, the heat fluxes for the convective cases decline with increasing shell thickness (despite the fact that Nu increases with Ra; see Fig. 4). Together, these traits imply that for a range of heat fluxes (0.04–0.06 W m$^{-2}$ for a melting-temperature viscosity of $10^{13}$ Pa s), there are *two solutions* for a given heat flux: one corresponding to a thin, conductive shell and the other to a thick, convective shell (see Fig. 1).

This figure has important implications for the thermal evolution of Europa. A given point in Fig. 5 corresponds to a true equilibrium on Europa only if the heat flux transported through the shell equals that supplied from Europa's oceanic/silicate interior. If the heat flux from Europa's oceanic/silicate interior differs from the flux that can be transported at a given ice-shell thickness, then the ice-shell thickness will change until the flux transported through the ice layer equals that supplied from below. For example, suppose the ice shell is 22-km thick, implying a heat flux through Europa's surface of 0.05 W m$^{-2}$ for $\eta_0 = 10^{13}$ Pa s (Fig. 5), and that tidal and radiogenic heating in the silicate interior supplies 0.03 W m$^{-2}$ to the ocean. The mismatch of heat fluxes will cause freezing at the base of the shell, which will continue until the shell becomes 55-km thick. At this point the heat flux through Europa's surface reaches that supplied from below (0.03 W m$^{-2}$; see Fig. 5) and freezing ceases—equilibrium is attained.

These arguments based on Fig. 5 suggest that, in either branch of the curves where heat flux decreases with increasing shell thickness, the ice shell is stable: for a given heat flux supplied by the interior, decreases in ice-shell thickness away from the equilibrium cause increases in the heat flux transported by the shell, cooling, and hence thickening, which returns the shell to its equilibrium thickness. Increases in shell thickness away from the equilibrium cause decreases in heat flux transported by the shell, warming, and hence thinning, which again returns the shell toward its equilibrium thickness. Fig. 5 also implies that variations in heat flux from the silicate interior can cause large changes in ice-shell thickness. If the heat flux from the silicate interior changes by 0.005 W m$^{-2}$, then the equilibrium thickness of a convective shell changes by ∼7 km and 20 km for $\eta_0 = 10^{13}$ and $10^{14}$ Pa s, respectively. In contrast, for a conductive ice shell, such a change in heat flux would cause only 1–2 km changes in the shell thickness.

Near the critical Rayleigh number, modest variations in heat flux can force the ice shell to switch between conductive and convective regimes, with consequent rapid changes in the ice-shell thickness. Imagine a conductive ice shell in equilibrium with a large, but slowly declining, heat flux supplied from the silicate layer. The system would occupy a point along the solid curve at the upper left of Fig. 5 and would slowly slide down the curve as the flux decreased. The shell thickens accordingly, remaining conductive as long as the thickness is less than 10, 20, or 40 km for melting-temperature viscosities of $10^{13}$, $10^{14}$, or $10^{15}$ Pa s, respectively. Once the shell reaches this critical thickness, however, a dilemma arises: the continually declining flux implies that the shell must continue to grow, but any further increase in the shell thickness causes an *increase*, not a decrease, in the flux transported through the ice layer. The system can no longer remain in equilibrium: it becomes convective, but because the convected flux greatly exceeds that supplied from below, the shell thickness increases rapidly until the system reaches a new equilibrium. For $\eta_0 = 10^{13}$ Pa s, the shell would jump from 10- to 35-km thickness, and for $\eta_0 = 10^{14}$ Pa s, the shell would jump from 19- to 65-km thickness. This constitutes a switch from the conductive to the convective solution at a given heat flux. Suppose now that the heat flux supplied to the base began to increase. The shell would

remain on the convective branch, thinning in response to the increased flux. Eventually, the shell would reach the critical Rayleigh number (at a thickness of ∼12, 22, or 45 km for melting-temperature viscosities of $10^{13}$, $10^{14}$, or $10^{15}$ Pa s, respectively); further thinning would force the shell into the conductive regime. However, this involves another crisis, because further thinning causes a *decrease*, not an increase, in the transported flux, forcing the system away from equilibrium (it cannot transport all of the flux supplied from below). The shell would then thin rapidly until a new equilibrium is attained. For $\eta_0 = 10^{13}$ Pa s, the shell would jump from 10- to 6-km thickness, and for $\eta_0 = 10^{14}$ Pa s, the shell would jump from 19- to 14-km thickness. Interestingly, the switches are asymmetric: conductive-to-convective switches involve much larger changes in the ice-shell thickness than convective-to-conductive switches.

We emphasize that these rapid conductive–convective switches result directly from the discontinuity in heat flux at $Ra_{cr}$ and, to our knowledge, have never been discussed to date for icy satellites. Many icy-satellite evolution models have been published, but these generally adopt Nu–Ra relationships (or equivalently, $F$–$\delta$ relationships) that are continuous at the critical Rayleigh number (e.g., Spohn and Schubert, 2003; Deschamps and Sotin, 2001; Hussmann et al., 2002; Hussmann and Spohn, 2004; Showman et al., 1997; Kirk and Stevenson, 1987; and others). Therefore, these studies explicitly preclude the conductive–convective switches discussed here.

Fig. 6 shows the heat flux through the bottom and top boundaries vs shell thickness for models that include tidal heating. For an internally heated ice shell, the basal flux $F_{hbl}$ depends more strongly on $\delta$ than for a shell without internal heating, which implies that variations in the flux supplied from the silicate interior cause smaller changes in shell thickness for a tidally heated shell (at constant tidal-flexing amplitude) than for a shell with zero tidal heating. For a melting-temperature viscosity of $10^{13}$ Pa s and tidal-flexing amplitude of $2 \times 10^{-5}$, for example, a basal heat-flux variation of 0.005 W m$^{-2}$ would cause a change in shell thickness of ∼1–4 km for a convecting shell, depending on the thickness (Fig. 6a). For a melting-temperature viscosity of $10^{14}$ Pa s and tidal-flexing amplitude of $1.1 \times 10^{-5}$, such a heat-flux perturbation would alter the shell thickness by ∼6 km (Fig. 6b). These thickness changes are a factor of ∼3–4 smaller than for a shell with no heating (Fig. 5).

The heat-flux jump at the critical Rayleigh number remains strong when tidal heating is included in the simulations (Fig. 6), which implies that conductive–convective transitions can occur in tidally heated shells just as they can in shells without tidal heating. If heat-flux variations from the silicate interior occur at constant ice-shell tidal-flexing amplitude, then Fig. 6 can describe evolutionary paths followed by Europa. For example, suppose Europa starts with a thin, conductive shell in equilibrium with a large basal-heat flux that gradually declines in time. The shell will gradually thicken in the conductive regime and then will switch

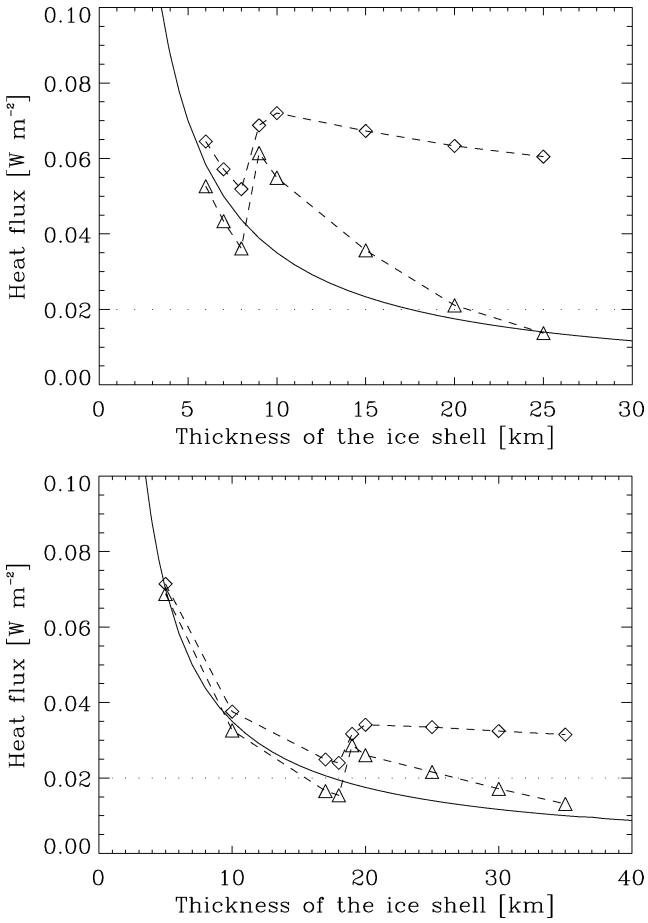


Fig. 6. Relation between the heat flux calculated in the hot boundary layer of the convective ice shell (triangles) and in the stagnant lid (diamonds) vs the thickness of the ice shell $\delta$ for simulations that include tidal heating in the ice shell. Solid curve shows the relationship between heat flux $F$ and $\delta$ for a conductive ice shell without internal heating. The radiogenic heat flux ranges from 0.005 to 0.020 W m$^{-2}$ (Melosh et al., 2004; Tobie et al., 2003). The maximum radiogenic heat flux is plotted in dashed line. The critical thickness of the ice shell, corresponding to the critical Rayleigh number, is ∼9 and ∼18 km in the top and bottom panels, respectively. (a) Melting-temperature viscosity is $10^{13}$ Pa s and the tidal-flexing amplitude is $\varepsilon_0 = 2.0 \times 10^{-5}$. (b) Melting-temperature viscosity is $10^{14}$ Pa s and the tidal flexing amplitude is $\varepsilon_0 = 1.1 \times 10^{-5}$.

rapidly to a much thicker convective regime (from 8- to 15-km thickness in Fig. 6a and from 18- to 31-km thickness in Fig. 6b). Similarly, a gradually increasing basal flux in the convective regime would lead to gradually thinner convective layers until a rapid switch to a much thinner conductive state occurred (from 9- to 5-km thickness in Fig. 6a and 19- to ∼11-km thickness in Fig. 6b).

Fig. 7 shows the dependence of the bottom and top fluxes transported by the ice shell on the tidal-flexing amplitude $\varepsilon_0$. Stronger tidal flexing leads to *increased* flux through Europa's surface but *decreased* flux into the ice layer from below. This behavior occurs because the ice shell is warmer when the tidal flexing is greater, which enhances loss of heat through the top surface and inhibits gain of heat through the bottom surface. At high Rayleigh numbers, the heat fluxes

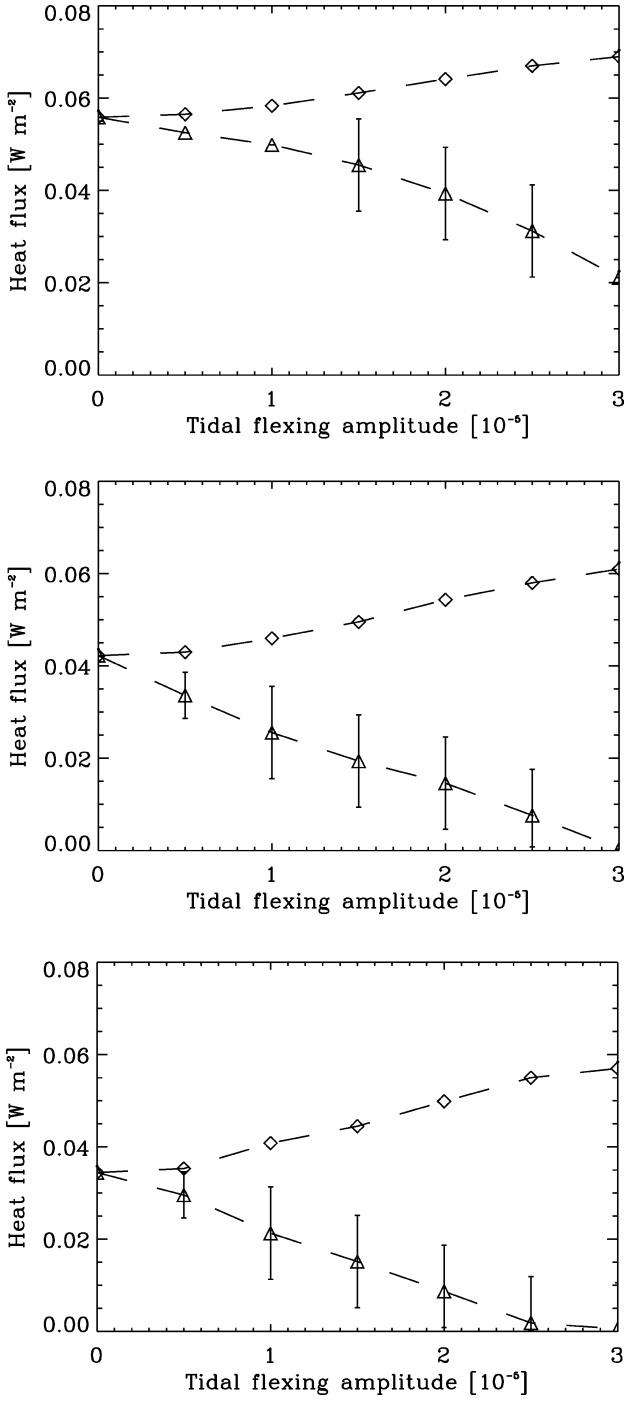


Fig. 7. Heat flux through the hot boundary layer of the convective ice shell (triangles) and stagnant lid (diamonds) versus the tidal flexing amplitude $\varepsilon_0$ for tidally heated ice shells. Increasing the orbital eccentricity and, consequently, the tidal-flexing amplitude decreases the ability of the ice shell to receive conducted heat from the interior of the satellite but increases the flux lost to space. Melting-temperature viscosity is $10^{13}$ Pa s. (a) Ice-shell thickness is 15 km; (b) ice-shell thickness is 30 km; (c) ice-shell thickness is 45 km.

into the base are time dependent, and the vertical bars illustrate the range of variation; the central point gives the time-averaged flux. The fluctuations generally occur on a convective overturn timescale, $\sim 10^4$–$10^5$ years, which is much

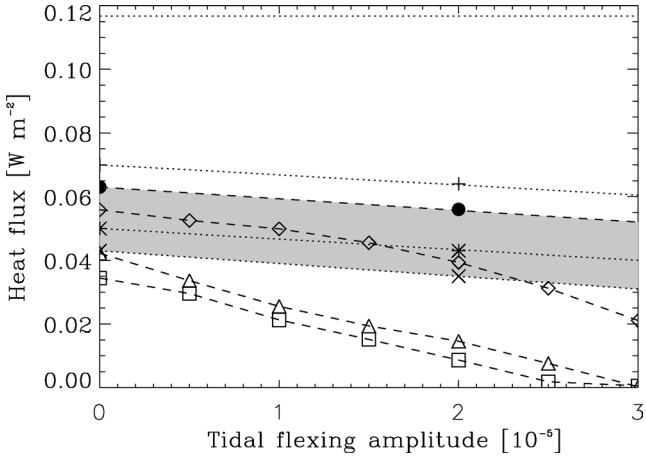


Fig. 8. Ice-shell thickness as a function of the heat flux from the interior of Europa and the tidal flexing amplitude of the ice shell for $\eta_0 = 10^{13}$ Pa s. Dashed and dotted lines correspond to convective and conductive solutions, respectively. Shown are 10-km convective (filled circles), 15-km convective (diamonds), 30-km convective (triangles), 45-km convective (squares), 8-km conductive (crosses), 7-km conductive (asterisks), and 5-km conductive (pluses) solutions. The dotted line at the top shows the conductive solution for a 3-km shell. The gray area denotes the region where both conductive and convective solutions exist for a given tidal-flexing amplitude and basal heat flux. Variations in these two parameters can cause rapid switches between conductive and convective states; see text.

smaller than typical orbital and thermal evolution timescales of $10^7$–$10^8$ years.

Fig. 8 summarizes the dependence of ice-shell thickness on the basal heat flux and ice-shell tidal-flexing amplitude for a range of conductive and convective simulations. The figure can be viewed as a contour plot of layer thickness; the dashed curves connect convective solutions for a given layer thickness, while dotted curves connect conductive solutions for a given layer thickness. The gray region denotes the parameter ranges where *both* conductive and convective solutions (with distinct ice-layer thicknesses) exist for a given tidal-flexing amplitude and basal heat flux. Above the gray region, only conductive solutions exist, and below the gray region, only convective solutions exist. The basal heat-flux (vertical axis) and ice-shell tidal-flexing amplitude (horizontal axis) can be viewed as parameters whose values are approximately independent of the ice-shell state; the magnitude of radiogenic/tidal heating and secular cooling of Europa's silicate interior determine the former, while Europa's eccentricity and tidal Love number determine the latter, e.g. (Ojakangas and Stevenson, 1989; Moore and Schubert, 2000). As these parameters vary, the location of the system on Fig. 8 changes, and Fig. 8 then shows how the ice-shell thickness varies in time (as long as the change in basal heat-flux and tidal-flexing amplitude occur with time constants of $>10^6$–$10^7$ years; see Section 2). Within the gray region, which of the solutions Europa occupies depends on prior history. If the system enters the gray region from above, the shell will remain conductive, but if the system enters the gray region from below, the system will remain convective. Large-amplitude switches between con-

ductive and convective states occur when the lower boundary of the gray region is crossed from above or the upper boundary of the gray region is crossed from below; these correspond to conductive-to-convective and convective-to-conductive switches, respectively. Conductive-to-convective switches cause increases in thickness ranging from ∼30 km at zero tidal heating to ∼8 km at a tidal-flexing amplitude of $\sim 2 \times 10^{-5}$.

Interestingly, Fig. 8 shows that fluctuations of the basal-heat flux at constant tidal-flexing amplitude are more likely than fluctuations of tidal-flexing amplitude at constant basal-heat flux to produce convective–conductive switches. In reality, fluctuations in basal-heat flux and tidal-flexing amplitude are probably correlated. Changes in basal-heat flux most plausibly result from changes in the tidal-heating rate in the silicate interior, and because the eccentricity is the primary factor controlling the tidal-heating rate, we expect that increases in basal-heat flux are probably accompanied by increases in ice-shell tidal-flexing amplitude (and vice versa). The system would then follow a path extending between lower-left and upper-right in Fig. 8. If Europa's interior composition matches carbonaceous chondrites, then the current radiogenic heat flux is about 0.01 $\mathrm{W\,m^{-2}}$, which is substantially below the parameter ranges that allow convective-conductive switches for $\eta_0 = 10^{13}$ Pa s; however, if the total silicate-layer heat flux (tidal + radiogenic) is several times the radiogenic value, then factor-of-two changes in tidal-flexing amplitude and basal-heat flux may result in large-amplitude switches between the conductive and convective states. Tidal-flexing amplitude is proportional to eccentricity, so such switches may occur if Europa undergoes factor-of-two changes in eccentricity. Models for the coupled orbital-geophysical evolution of the Galilean satellites show that two-fold changes in eccentricity are quite plausible (e.g., Ojakangas and Stevenson, 1986; Showman and Malhotra, 1997; Showman et al., 1997; Hussmann and Spohn, 2004), which suggests the plausibility of large-amplitude conductive–convective switches.

Even in the absence of convective–conductive switches, Fig. 8 shows the sensitivity of ice-shell thickness to fluctuations in heating. A variation in $\varepsilon_0$ from 0 to $2.4 \times 10^{-5}$ changes the ice-shell thickness by 30 km for a fixed basal-heat flux of 0.035 $\mathrm{W\,m^{-2}}$. A variation of the tidal flexing amplitude $\varepsilon_0$ from 1.0 to $1.5 \times 10^{-5}$, and a simultaneous increase of the heat flux from the rocky interior from 0.021 to 0.050 $\mathrm{W\,m^{-2}}$, produce a variation in thickness of 30 km.

The time scale of the conductive–convective switches can be estimated as follows. When a switch occurs, the mismatch between the flux that can be transported through the ice shell and the flux supplied from below is $\Delta F \sim 0.02\ \mathrm{W\,m^{-2}}$ (Figs. 5, 6, and 8). This mismatch causes melting or freezing. The resulting timescale for the ice shell to achieve a new equilibrium is $\tau \sim L\rho\Delta\delta/\Delta F$, where $\Delta\delta$ is the variation in thickness and $L = 3 \times 10^5\ \mathrm{J\,kg^{-1}}$ is the latent heat. For a typical value of $\Delta\delta \sim 10$ km, the equilibration timescale is $\tau \sim 5 \times 10^6$ years.

We find that the maximum heat flux that can be transported by convection is $F_{\max} \sim 0.06\ \mathrm{W}m^{-2}$ for $\eta_0 = 10^{13}$ Pa s, $F_{\max} \sim 0.025\ \mathrm{W\,m^{-2}}$ for $\eta_0 = 10^{14}$ Pa s, and $F_{\max} \sim 0.015\ \mathrm{W\,m^{-2}}$ for $\eta_0 = 10^{15}$ Pa s (Figs. 5 and 6). These maximum fluxes are largely independent of tidal-heating rate. For higher values of the heat flux, convection cannot occur in the ice shell and the heat is transported by thermal conduction. This conclusion agrees with the results of Showman and Han (2004).

The minimum heat flux from the interior of Europa is the heat of radiogenic decay, which for carbonaceous–chondritic abundances of Europa's rocky portion is just under 0.01 $\mathrm{W\,m^{-2}}$ (Spohn and Schubert, 2003). Our results show that, if no tidal heating occurs, the ice shell would eventually freeze if the melting-temperature viscosity is $10^{13}$ or $10^{14}$ Pa s. For a melting-temperature viscosity of $10^{15}$ Pa s, however, the shell can never freeze even if tidal-heating is zero in both the ice shell and silicate interior. As discussed previously, however, plausible tidal-heating rates imply that the shell does not freeze completely even at melting-temperature viscosities of $10^{13}$ or $10^{14}$ Pa s; this result is consistent with the results of many previous studies (e.g., Spohn and Schubert, 2003; Tobie et al., 2003; Hussmann et al., 2002; Deschamps and Sotin, 2001).

### 3.4. Satellite expansion/contraction caused by conductive–convective switch

The large variations in ice-shell thickness during a switch between conductive and convective configurations can cause rapid radial expansion of Europa. A refreezing of 10 km of the ice shell causes a radial expansion of ∼1 km, corresponding to a fractional satellite volume change of $2 \times 10^{-3}$ and a global, linear extensional strain of $6 \times 10^{-4}$ at the surface. Such an expansion would fracture the surface and generate $4 \times 10^4$ km$^2$ of new surface area, which could potentially result in the formation of bands or other extensional tectonic structures. Here we estimate the stress in the ice shell during the radial expansion. The stress as a function of the ice-shell temperature is calculated using the flow law of Eq. (7) in the generalized Maxwellian viscoelastic equation

$$\dot{\varepsilon} = \frac{\dot{\sigma}}{\mu} + \frac{\sigma}{\eta} + A\frac{\sigma^n}{d^p}\exp\left(-\frac{Q^*}{RT}\right), \tag{13}$$

where $\mu = 4 \times 10^9$ Pa is the rigidity, $\eta$ is the Newtonian viscosity, and the third term represents non-Newtonian deformation. The composite constitutive steady-state creep law proposed by Goldsby and Kohlstedt (2001) show that, at Europa's surface, dislocation and diffusion creep are predominant, so the final term here represents dislocation creep with $n = 4$ and $Q^* = 60\ \mathrm{kJ\,mol^{-1}}$ (see Table 2). We expect that satellite expansion does not depend on ice-shell stress, so we independently specify $\dot{\varepsilon}$ as a function of time (to represent satellite expansion) and solve the differential equation to find the maximum value of stress at a given temperature

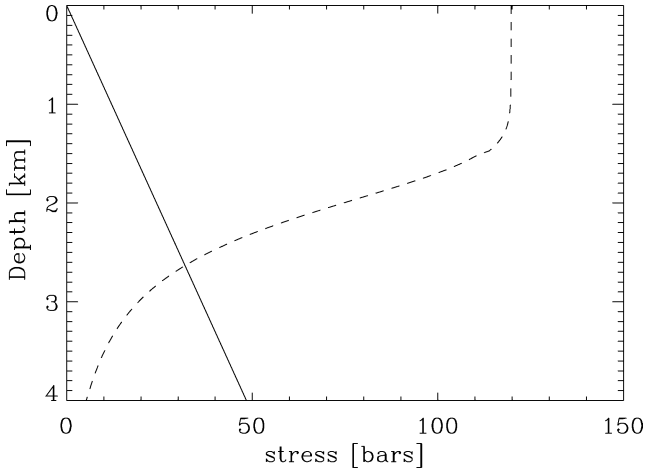


Fig. 9. Stress and fracture depth of open cracks during the radial expansion of Europa for a temperature gradient of 30 K km$^{-1}$. The rigidity of the ice is $4 \times 10^9$ Pa, the water ice viscosity $\eta_0 = 10^{13}$ Pa s, and the thermal conductivity is $k_{av} = 3.4$ W m$^{-1}$ K$^{-1}$. The heat from the interior of Europa is 0.045 W m$^{-2}$. The refreezing time scale is $7 \times 10^6$ yr and the fractional volume expansion is $9 \times 10^{-3}$, corresponding to a 30-km thickening of the ice shell. The dashed line shows the stress caused by the expansion and the solid line gives the hydrostatic pressure. The maximum depth of open fractures is given when the hydrostatic pressure equal the extensional stress.

(Showman et al., 1997). We write $\dot{\varepsilon}$ with a Gaussian form

$$\dot{\varepsilon} = \frac{\Delta V}{3V} \frac{1}{\tau\sqrt{\pi}} \exp\left(-\frac{(t-3\tau)^2}{\tau^2}\right), \tag{14}$$

where $t$ is time, $\tau$ is the characteristic expansion time scale, and $\Delta V/V$ is the fractional volume expansion. Fig. 9 shows the maximum stress vs depth assuming that $\tau = 7 \times 10^6$ years and $\Delta V/V = 9 \times 10^{-3}$. This corresponds to a ice-shell thickness change of 45 km, which is an upper limit for a conductive–convective transition (Fig. 8). We adopt a vertical temperature gradient of 13.2 K km$^{-1}$ (assumed constant), which, for a thermal conductivity $k = 3.4$ W m$^{-1}$ K$^{-1}$, corresponds to a surface heat flux of 0.045 W m$^{-2}$. The stress (dashed curve) peaks at ∼120 bar at the surface and declines rapidly with depth. The maximum depth of open extension fractures is ∼2.7 km (corresponding to the intersection of the hydrostatic pressure, shown in solid, with the stress). This fracture depth may be sufficient to allow ascent of warm ice and the formation of bands.

## 4. Conclusions

We investigated the response of conductive and convective ice shells on Europa to changes of heat production in the ice shell and silicate mantle, with the aim of placing constraints on Europa's geological history and long-term thermal evolution. We performed numerical simulations of subsolidus convection with temperature-dependent Newtonian viscosity and a range of tidal-heating rates, ice-shell thicknesses, and melting-temperature viscosities; the viscosity contrast was chosen to maintain the convection in the stagnant–lid regime. Our results support earlier conclusions (McKinnon, 1999) that convection occurs in ice shells thicker than ∼10–20 km for melting-temperature viscosities of $10^{13}$–$10^{14}$ Pa s. Two transitions in the convective behavior occur as the Rayleigh number increases. The first transition happens at $Ra \sim 1 \times 10^7$–$1 \times 10^8$ with a change from steady to time-dependent convection (the exact Ra depending on the tidal-heating rate). The second transition occurs at $Ra \sim 10^9$ with a shift of the Nusselt-number scaling exponent, $\beta$ (from the relationship $Nu = \alpha Ra^{\beta}\theta^{\gamma}$), from ∼1/5 to 1/3. In agreement with Showman and Han (2004), we find that the maximum heat flux than can be convected is ∼0.06 W m$^{-2}$, depending on the ice viscosity and tidal-heating rate. For higher heat fluxes, convection cannot occur in the ice shell and the heat is transported by thermal conduction.

Intriguingly, we find that, at the critical Rayleigh number, convection jumps immediately into a finite-amplitude state, in agreement with laboratory results by Stengel et al. (1982) for a fluid with strongly temperature-dependent viscosity. This result implies that, for a range of basal-heat fluxes and ice-shell tidal-flexing amplitudes relevant to Europa, *two equilibrium states* exist: one for a thin, conductive ice shell and the other for a thick, convective ice shell. To our knowledge this phenomenon has never previously been discussed in the icy-satellite context. The primary relevance for Europa is that, under appropriate conditions, small changes in heat flux or tidal-flexing amplitude can force the ice shell to switch between these two states, leading to large—and *rapid*—changes in the ice-shell thickness. Global expansion or contraction of Europa would result, depending on whether the shell thickened or thinned. Conductive-to-convective switches causes ice-shell thickening of ∼8–30 km, depending on the tidal-heating rate, whereas convective-to-conductive switches lead to thinning of ∼5–10 km. The timescale of these conductive–convective switches, ∼5–10 Myr, is much less than probable timescales for the orbital fluctuations ($10^8$ years) and changes in radiogenic heat flux ($10^9$ years) that allow the switches to occur. The rapidity of these switches implies that stress buildup, hence extensive fracture, of Europa's surface would occur during such a switch; in contrast, gradual ∼$10^8$-year changes in the ice-shell thickness would allow the expansion or contraction to be accommodated by viscous deformation rather than fracture.

Several studies have shown that Europa's resurfacing has shifted from a tectonic regime (i.e., ridge-building) to chaos and lenticulae formation throughout the course of the ∼50 Myr observational record (Figueredo and Greeley, 2004; Greeley et al., 2000; Kadel et al., 2000; Prockter et al., 1999; Pappalardo et al., 1999). Based on the interpretation that chaos and lenticulae result from convection in the ice shell (e.g., Collins et al., 2000), several of these authors have interpreted this shift as evidence for a thickening of the ice shell with time, resulting in the onset of convection sometime within the past ∼50 Myr

(see Pappalardo et al., 1999 for a review). A possible dilemma in explaining chaos is that, if convection has only just initiated, one might expect the convection to be relatively low-amplitude, which makes it difficult to understand how surface disruption would result from the convection. Our simulations provide a mechanism for producing a rapid ($\sim 10^7$ year) shift from a conductive state to a high-amplitude, vigorously convecting state potentially capable of forming chaos. Furthermore, the rapidity of the shift would allow lithospheric fracture and band formation, which is broadly consistent with the inference that bands are often intermediate in age between the ridged plains and chaos (Figueredo and Greeley, 2004). Finally, our model shows that, under the right conditions, the shift from conductive to vigorous–convective states can occur with only modest perturbations in the basal heat flux and tidal-flexing amplitude. If Europa's heat flux varies cyclically in time (Ojakangas and Stevenson, 1986; Hussmann and Spohn, 2004), such switches could occur repeatedly during Europa's history.

Even if no such switches occur, our simulations describe how the ice-shell thickness responds to changes in the heat flux and tidal-heating rate. Because of the weak dependence of the heat flux on the thickness, a convective ice shell responds to modest variations in heat flux with large variations in thickness. In a convective ice shell without internal heating in the $\beta = 1/5$ convective regime, a variation of heat flux of 0.01 $\mathrm{W\,m^{-2}}$ involves changes of thickness $\geqslant$10 km. In contrast, large variations of heat flux involves relatively small variations of thickness in a conductive ice shell. Tidal heating in the ice shell lessens the sensitivity of ice-shell thickness to variations in basal heat flux, however.

In conclusion, we have shown that variations in heat production in the interior of Europa can produce large variation in thickness of a convective ice shell. Moreover, modest variation in the heat flux supplied from below can produce repeated switches from a conductive to a convective configuration of the ice shell during its thermal history, with rapid and large variations in thickness. Based on interpretations for how features such as chaos, ridges and bands are formed, several authors have suggested that Europa's ice shell has recently undergone changes in thickness. Our model provides a mechanism for such changes to occur.

## Acknowledgments

We thank Paul Geissler, Lijie Han, Gabriel Tobie, and Hirdy Miyamoto. We are grateful to Hauke Hussmann and William B. Moore. This project was supported by the Italian Space Agency (ASI) and the NASA PG&G program through Grant NNG04GI46G to A.P.S.

## References

Barr, A.C., Pappalardo, R.T., 2003. Numerical simulations of non-Newtonian convection in ice: Application to Europa. Lunar Planet. Sci. XXXIV. Abstracts 1477.

Cassen, P., Reynolds, R.T., Peale, S.J., 1979. Is there liquid water on Europa. Geophys. Res. Lett. 6, 731–734.

Collins, G.C., Head, J.W., Pappalardo, R.T., Spaun, N.A., 1999. Evaluating models for the formation of chaotic terrain on Europa. Lunar Planet. Sci. XXX. Abstracts 1477.

Collins, G.C., Head, J.W., Pappalardo, R.T., Spaun, N.A., 2000. Evaluation of models for the formation of chaotic terrain on Europa. J. Geophys. Res. 105, 1709–1716.

Davaille, A., Jaupart, C., 1993. Transient high-Rayleigh-number thermal convection with large viscosity variations. J. Fluid Mech. 253, 141–166.

Deschamps, F., Sotin, C., 2001. Thermal convection in the outer shell of large satellites. J. Geophys. Res. 106, 5107–5121.

Dropkin, D., Somerscales, E., 1965. Heat transfer by natural convection in liquids confined by two parallel plates which are inclined at various angles with respect to the horizontal. J. Heat Transfer 87, 77–84.

Dumoulin, C., Doin, M.P., Fleitout, L., 1999. Heat transport in stagnant lid convection with temperature- and pressure-dependent Newtonian or non-Newtonian rheology. J. Geophys. Res. 104, 12759–12777.

Durham, W.B., Kirby, S.H., Stern, L.A., 1997. Creep of water ices at planetary conditions: A compilation. J. Geophys. Res. 102, 16293–16302.

Figueredo, P.H., Chuang, F.C., Rathbun, J., Kirk, R.L., Greeley, R., 2002. Geology and origin of Europa's "Mitten" feature (Murias Chaos). J. Geophys. Res. 107. 2-1.

Figueredo, P.H., Greeley, R., 2004. Resurfacing history of Europa from pole-to-pole geologimapping. Icarus 167, 287–312.

Fowler, A.C., 1985. Fast thermoviscous convection. Stud. Appl. Math. 72, 189–219.

Goldsby, D.L., Kohlstedt, D.l., 2001. Superplastic deformation of ice: Experimental observations. J. Geophys. Res. 106, 11017–11030.

Goldstein, R.J., Chiang, H.D., See, D.L., 1990. High-Rayleigh number convection in a horizontal enclosure. J. Fluid Mech. 213, 111–126.

Greeley, R., Collins, G.C., Spaun, N.A., Sullivan, R.J., Moore, J.M., Senske, D.A., Tufts, B.R., Johnson, T.V., Belton, M.J.S., Tanaka, K.L., 2000. Geologic mapping of Europa. J. Geophys. Res. 105, 22559–22578.

Greenberg, R., 1982. Orbital evolution of the Galilean satellites. In: Morrison, D. (Ed.), Satellites of Jupiter. University of Arizona Press, AZ, pp. 65–92.

Greenberg, R., Geissler, P., Hoppa, G., Tufts, B.R., Durda, D.D., Pappalardo, R., Head, J.W., Greeley, R., Sullivan, R., Carr, M.H., 1998. Tectonic processes on Europa: Tidal stresses, mechanical response, and visible features. Icarus 135, 64–78.

Greenberg, R., Hoppa, G.V., Tufts, B.R., Geissler, P., Riley, J., Kadel, S., 1999. Chaos on Europa. Icarus 141, 263–286.

Greenberg, R., Geissler, P., Tufts, B.R., Hoppa, G.V., 2000. Habitability of Europa's crust: The role of tidal–tectonic processes. J. Geophys. Res. 105, 17551–17562.

Greenberg, R., Leake, M.A., Hoppa, G.V., Tufts, B.R., 2003. Pits and uplifts on Europa. Icarus 161, 102–126.

Head, J.W., Pappalardo, R.T., 1999. Brine mobilization during lithospheric heating on Europa: Implications for formation of chaos terrain, lenticula texture, and color variations. J. Geophys. Res. 104, 27143–27156.

Howard, L.N., 1964. Convection at high Rayleigh number. In: Gortler, H. (Ed.), Proceeding of the 11th International Congress on Applied Mechanics. Springer-Verlag, New York, pp. 1109–1115.

Hussmann, H., Spohn, T., 2004. Thermal-orbital evolution of Io and Europa. Icarus 171, 391–410.

Hussmann, H., Spohn, T., Wieczerkowski, K., 2002. Thermal equilibrium states of Europa's ice shell: Implications for internal ocean thickness and surface heat flow. Icarus 156, 143–151.

Kadel, S.D., Chuang, F.C., Greeley, R., Moore, J.M., 2000. Geological history of the Tyre region of Europa: A regional perspective on europan surface features and ice thickness. J. Geophys. Res. 105, 22656–22669.

Kargel, J.S., 1991. Brine volcanism and the interior structures of asteroids and icy satellites. Icarus 94, 368–390.

King, S.D., Raefsky, A., Hager, B.H., 1990. ConMan: Vectorizing a finite element code for incompressible two dimensional convection in the Earth mantle. Phys. Earth Int. 59, 195–207.

Kirk, R.L., Stevenson, D.J., 1987. Thermal evolution of a differentiated Ganymede and implications for surface features. Icarus 69, 91–134.

Kivelson, M.G., Khurana, K.K., Russell, C.T., Volwerk, M., Walker, R.J., Zimmer, C., 2000. Galileo Magnetometer measurements: A stronger case for a subsurface ocean at Europa. Science 289, 1340–1343.

McKinnon, W.B., 1998. Geodynamics of icy satellites. In: Schmitt, B., de Bergh, C., Festou, M. (Eds.), Solar System Ices. Kluwer Academic, Dordrecht, pp. 525–550.

McKinnon, W.B., 1999. Convective instability in Europa's floating ice shell. Geophys. Res. Lett. 26, 951–954.

Melosh, H.J., Turtle, E.P., 2004. Ridges on Europa: Origin by incremental ice-wedging. Lunar Planet. Sci. XXXV. Abstract 2029 [CD-ROM].

Melosh, H.J., Ekholm, A.G., Showman, A.P., Lorenz, R.D., 2004. The temperature of Europa's subsurface ocean. Icarus 168, 498–502.

Moore, W.B., Schubert, G., 2000. The tidal response of Europa. Icarus 147, 317–319.

Moresi, L.N., Solomatov, V.S., 1995. Numerical investigation of 2D convection with extremely large viscosity variations. Phys. Fluids 7, 2154–2162.

Moresi, L.N., Zhong, S., Gurnis, M., 1996. The accuracy of finite element solutions of Stokes' flow with strongly varying viscosity. Phys. Earth Planet. Int. 97, 83–94.

Morris, S., Canright, 1984. A boundary-layer analysis of Bernard convection in a fluid of strongly temperature-dependent viscosity. Phys. Earth Planet Int. 36, 355–373.

Nimmo, F., Gaidos, E., 2002. Strike-slip motion and double ridge formation on Europa. J. Geophys. Res. 107. 5021.

O'Brien, D.P., Geissler, P., Greenberg, R., 2002. A melt-through model for chaos formation on Europa. Icarus 156, 152–161.

Ojakangas, G.W., Stevenson, D.J., 1986. Episodic volcanism of tidally heated satellites with application to Io. Icarus 66, 341–358.

Ojakangas, G.W., Stevenson, D.J., 1989. Thermal state of an ice shell on Europa. Icarus 81, 220–241.

Pappalardo, R.T., Head, J.W., Greeley, R., Sullivan, R.J., Pilcher, C., Schubert, G., Moore, W.B., Carr, M.H., Moore, J.M., Belton, M.J.S., 1998. Geological evidence for solid-state convection in Europa's ice shell. Nature 391, 365.

Pappalardo, R.T., 31 colleagues, 1999. Does Europa have a subsurface ocean? Evaluation of the geological evidence. J. Geophys. Res. 104, 24015–24056.

Prockter, L.M., Antman, A.M., Pappalardo, R.T., Head, J.W., Collins, G.C., 1999. Europa: Stratigraphy and geological history of the anti-jovian region from Galileo E14 solid-state imaging data. J. Geophys. Res. 104, 16531–16566.

Roberts, G.O., 1979. Fast isoviscous Bernard convection. Geophys. Astrophys. Fluid Dyn. 12, 235–272.

Ross, M.N., Schubert, G., 1987. Tidal heating in an internal ocean model of Europa. Nature 325, 133.

Schenk, P.M., 2002. Thickness constraints on the icy shells of the Galilean satellites from a comparison of crater shaper. Nature 417, 419–421.

Schubert, G., Turcotte, D.L., Olson, P., 2001. Mantle Convection in the Earth and Planets. Cambridge Univ. Press, New York.

Showman, A.P., Han, L., 2004. Numerical simulations of convection in Europa's ice shell: Implications for surface features. J. Geophys. Res. 109. 1010.

Showman, A.P., Malhotra, R., 1997. Tidal evolution into the Laplace resonance and the resurfacing of Ganymede. Icarus 127, 93–111.

Showman, A.P., Stevenson, D.J., Malhotra, R., 1997. Coupled orbital and thermal evolution of Ganymede. Icarus 129, 367–383.

Solomatov, V.S., 1995. Scaling of temperature- and stress-dependent viscosity convection. Phys. Fluids 7, 266–274.

Solomatov, V.S., Moresi, L.N., 2000. Scaling of time-dependent stagnant lid convection: Application to small-scale convection on Earth and other terrestrial planets. J. Geophys. Res. 105, 21795–21817.

Somerscales, E.F.G., Gazda, I.W., 1986. Thermal Convection in High Prandtl Number Liquids at High Rayleigh Numbers. Rensselaer Polytech. Inst., ME Rep. HT-5. Troy, NY.

Sotin, C., Head, J.W., Tobie, G., 2002. Europa: Tidal heating of upwelling thermal plumes and the origin of lenticulae and chaos melting. Geophys. Res. Lett. 29. 74-1.

Spohn, T., Schubert, G., 2003. Oceans in the icy Galilean satellites of Jupiter? Icarus 161, 456–467.

Stengel, K.C., Oliver, D.S., Booker, J.R., 1982. Onset of convection in a variable viscosity fluid. J. Fluid Mech. 120, 411–431.

Tobie, G., Choblet, G., Sotin, C., 2003. Tidally heated convection: Constraints on Europa's ice shell thickness. J. Geophys. Res. 108, 5124.

Turcotte, D.L., Oxburgh, E.R., 1967. Finite amplitude convective cells and continental drifts. J. Fluid Mech. 28, 29–42.

Turtle, E., Ivanov, B., 2002. Numerical simulations of crater excavation and collapse on Europa: Implications for the ice thickness. Lunar Planet. Sci. XXXIII. Abstracts 1431.

Wang, H., Stevenson, D.J., 2000. Convection and internal melting of Europa's ice shell. Lunar Planet. Sci. XXXI. Abstracts 1293.

Williams, K.K., Greeley, R., 1998. Estimates of ice thickness in the Conamara Chaos region of Europa. Geophys. Res. Lett. 25, 4273–4276.